Electronic Supplementary Material (ESI) for Sustainable Energy & Fuels.

Supplementary Material

Nanoporous Carbon Doped Ceria Bismuth Oxide Solid Solution for Photocatalytic Water Splitting

Kahkashan Ansari[a], Saurabh Dalela[b], Sudhish Kumar[c] and Neelu Chouhan[a*]

[a] Department of Pure and Applied Chemistry, University of Kota, MBS Road, Kota-324005 (India)

[b] Department of Pure and Applied Physics, University of Kota, MBS Road, Kota-324005 (India)

[c] Department of Physics, Mohanlal Sukhadia University, Udaipur-323002 (India)

*Corresponding author : Phone: 91-0744-2471742 and Fax : +91-744-2472960 e-mail:

neeluchouhan@uok.ac.in

(a)

(b)

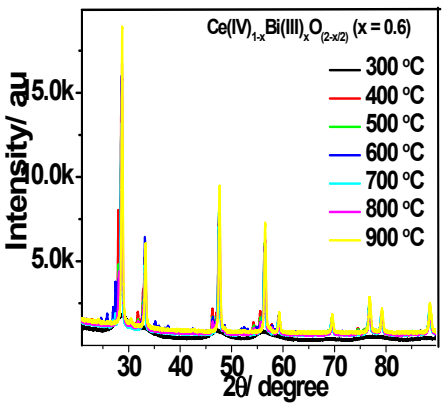

(b)

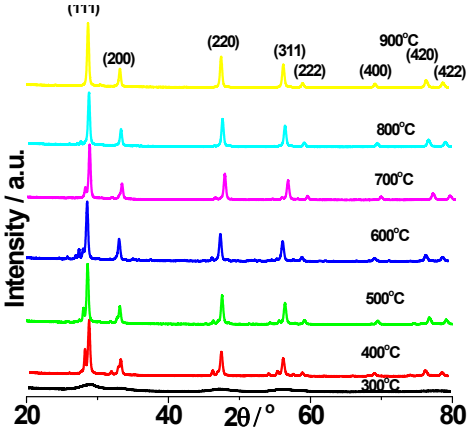

(c)

Figure S1. Solid solutions CBO, synthesized at varying temperatures i. e. 300, 400, 500,600, 700, 800 and 900°C with (a) and (b) physical appearance (c) and (d) their XRD patterns observed at different 2θ angles with raising temperature.

SEM IMAGES

(i). Pure compound CBO

(a) 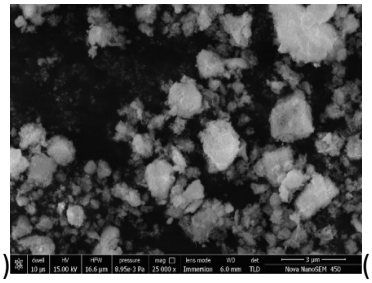
(b) 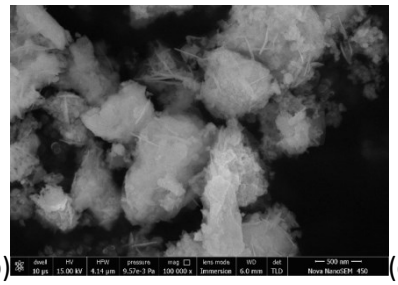
(c) 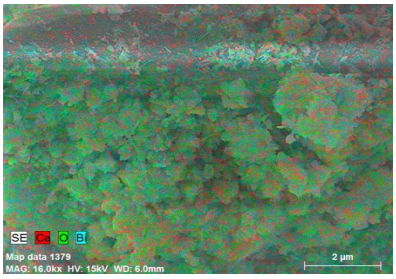

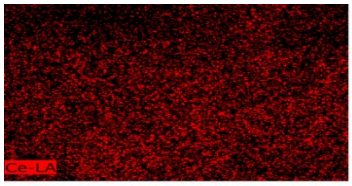

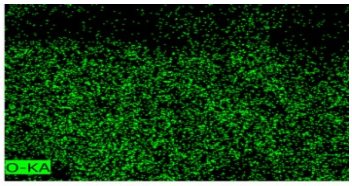

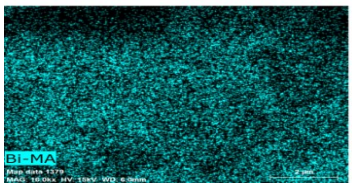

(e)

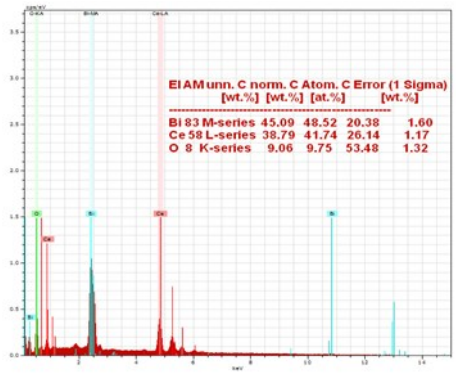

(e)

(ii). 2% C doped-CBO

(a) 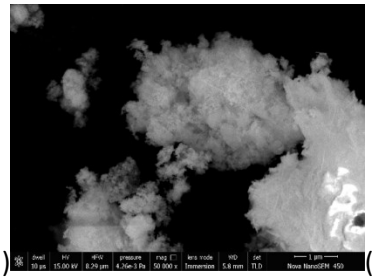
(b) 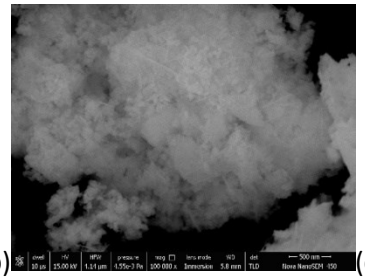
(c) 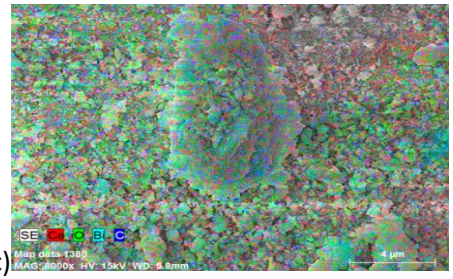

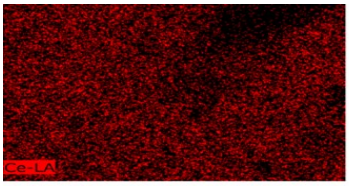

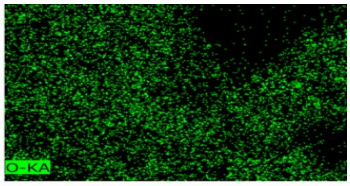

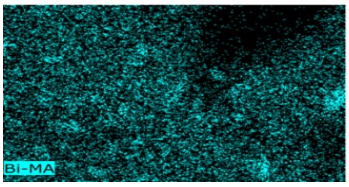

(d)
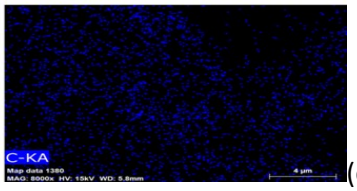

(e)

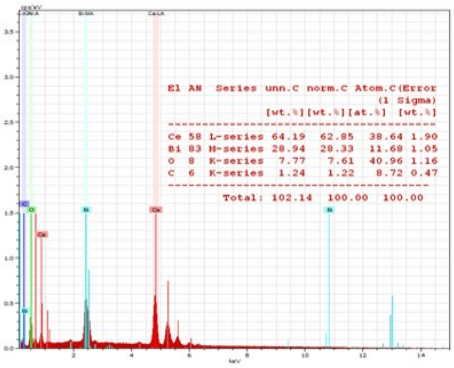

(iii). 4% C doped-CBO

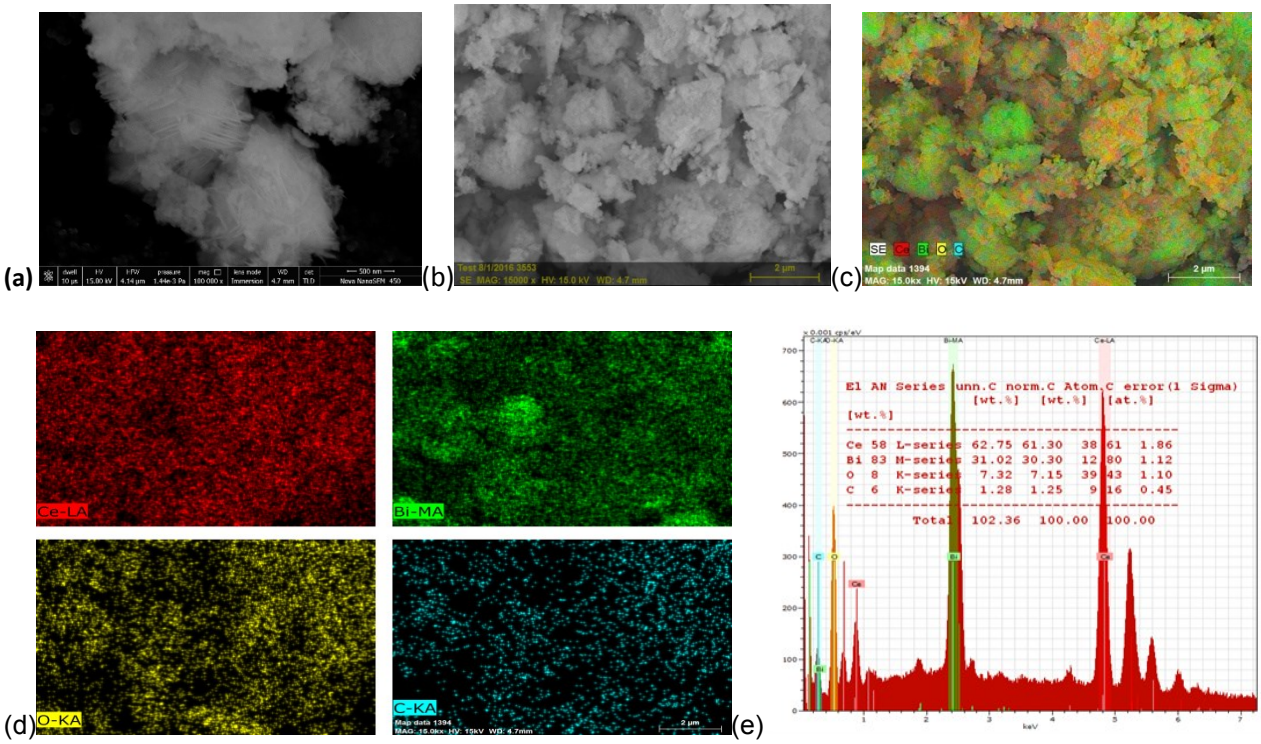

(iv). 6% C doped -CBO

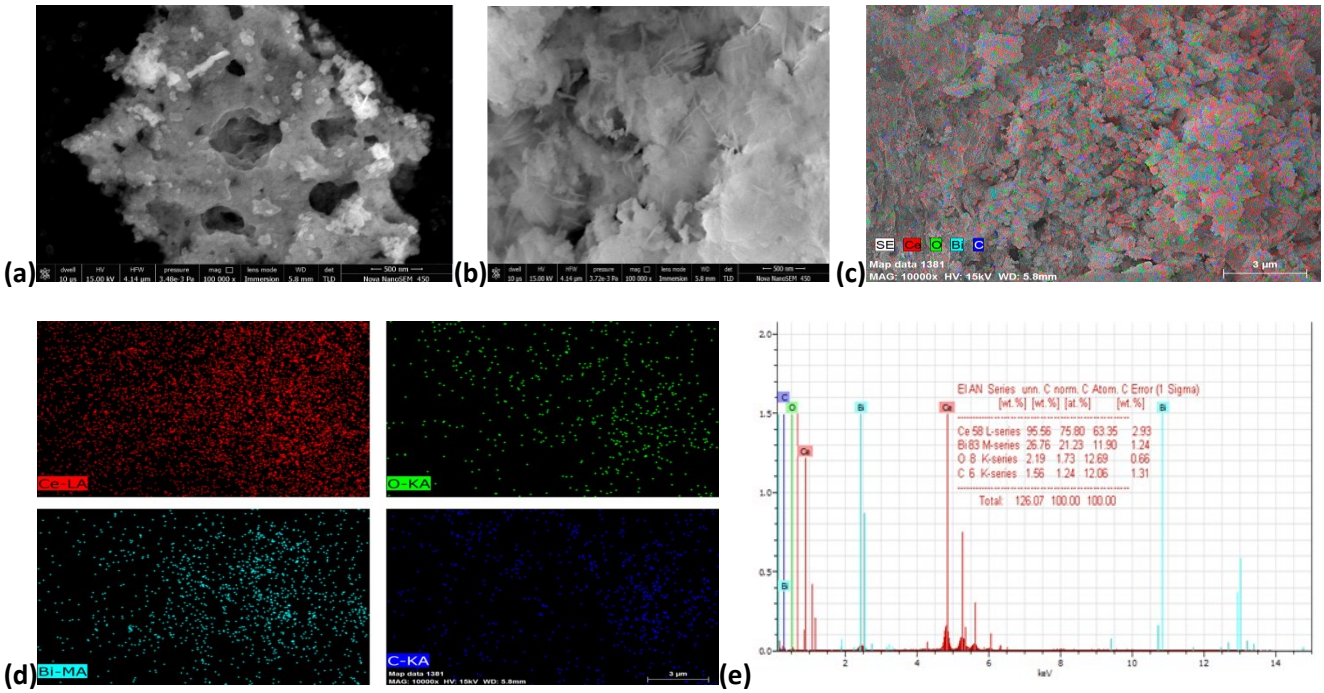

(v). 8% C doped -CBO

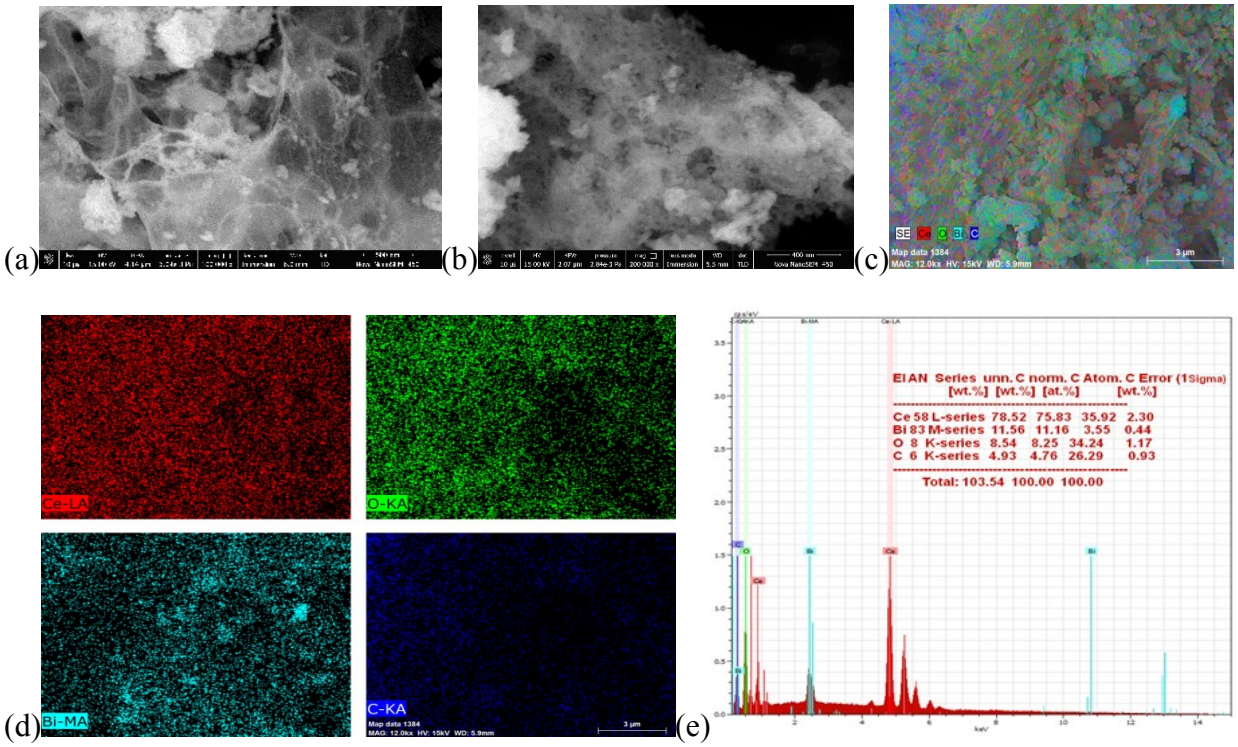

(vi). 10% C doped -CBO

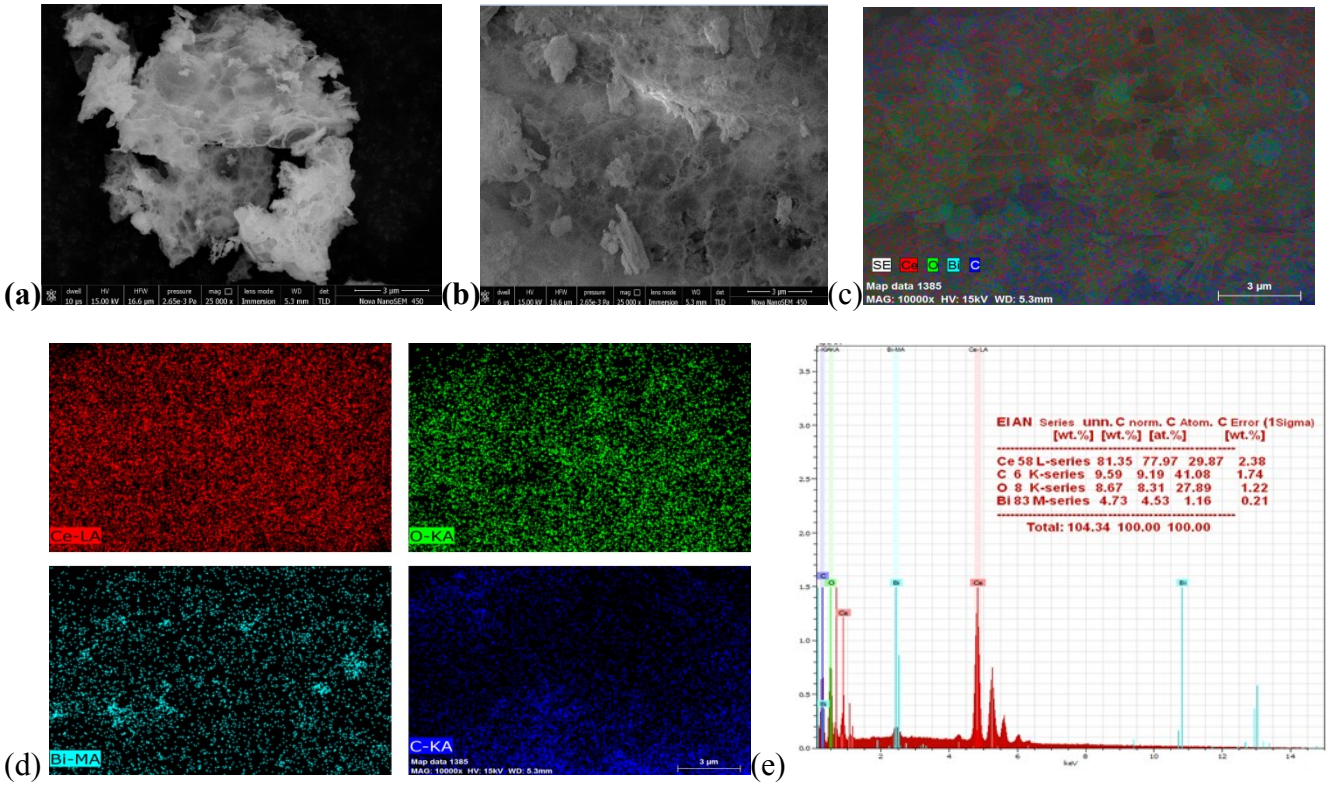

Figure S2 SEM images and corresponding EDX elemental mapping with percentage composition of the compounds, as depicted by the EDX profile of the pure CBO and 2%, 4%, 6%, 8% and 10%- carbon doped CBO samples.

I: Pure CBO

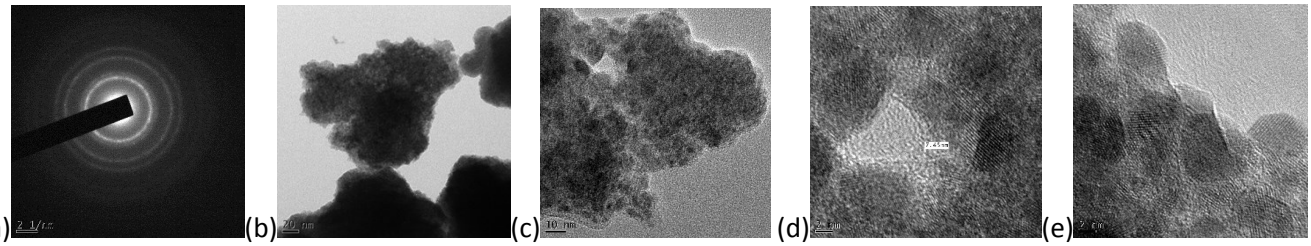

II: 2% C-doped CBO

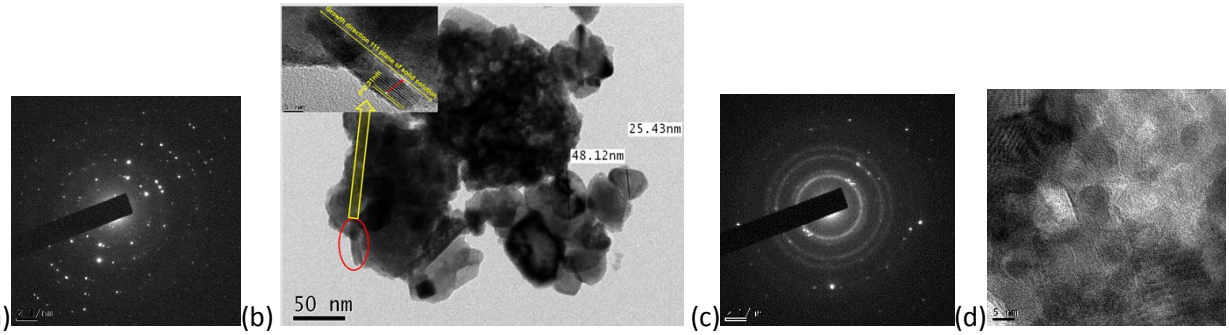

III: 4% C-doped CBO

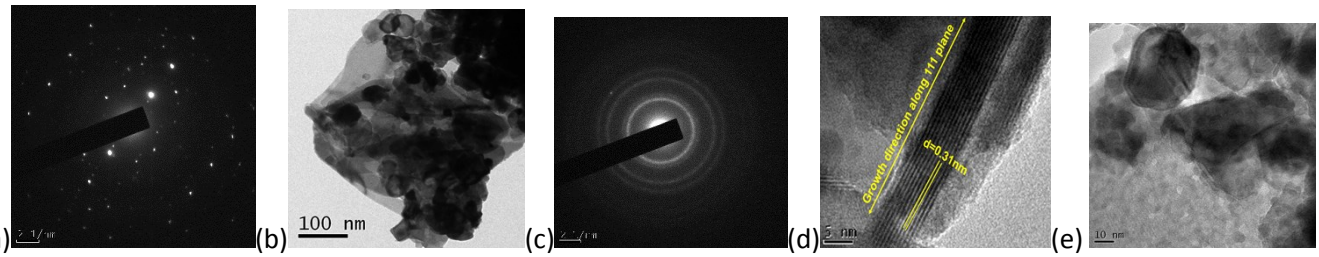

IV: 6% C-doped CBO

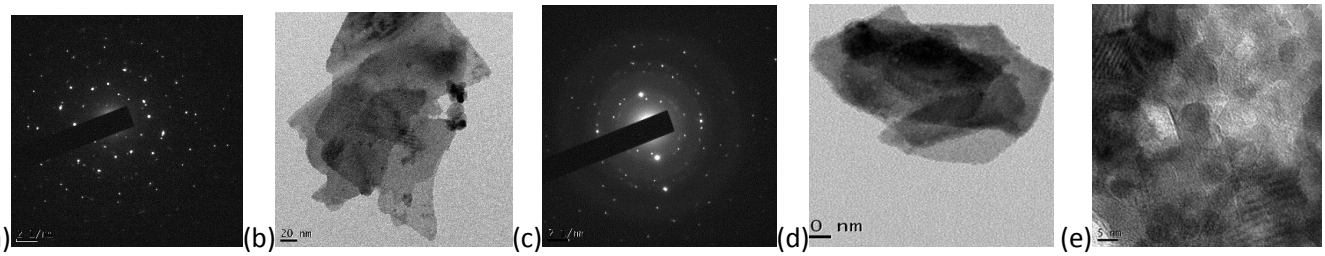

IV: 8% C-doped CBO

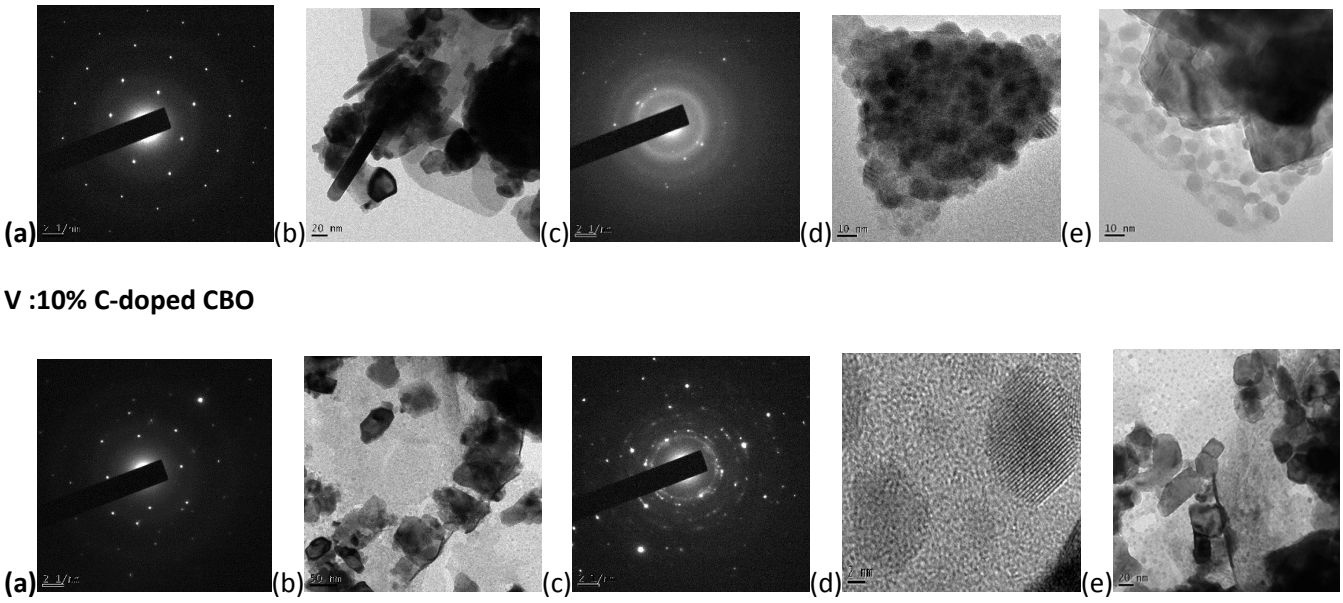

Figure S3. HRTEM images and corresponding SAED patterns of the pure CBO and C-doped CBO solid solutions.

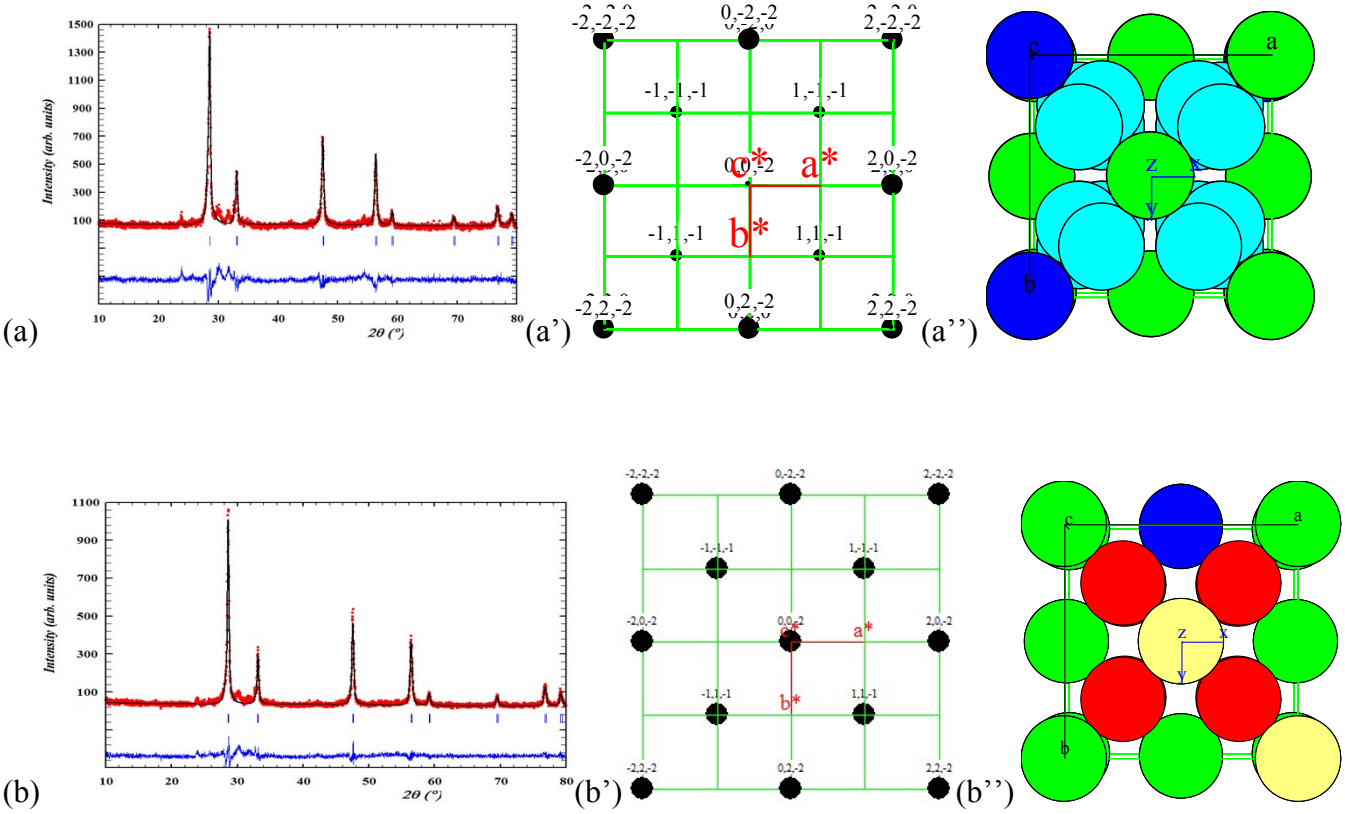

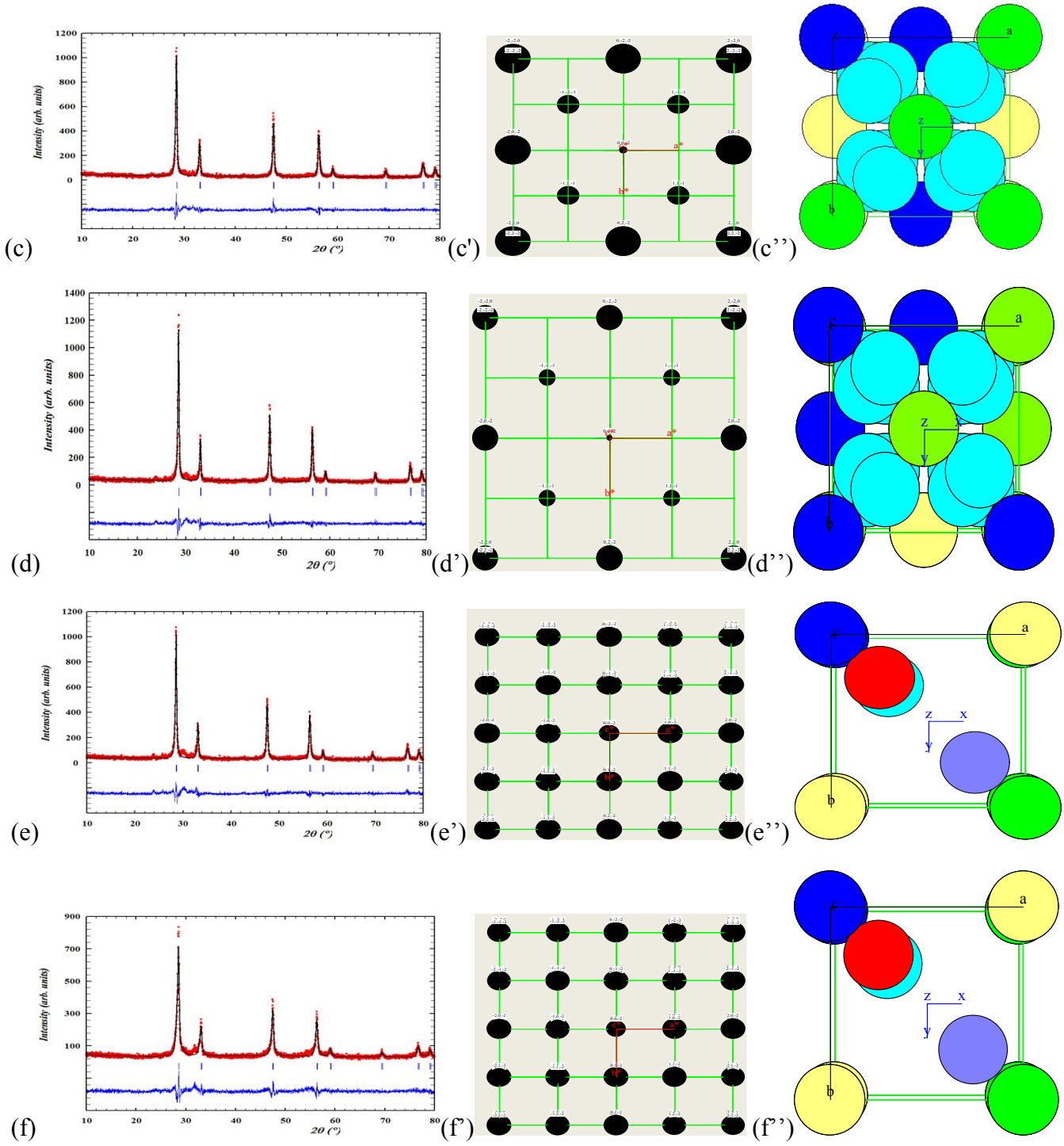

Figure S4 Rietveld refinement-based visual fit to X-ray diffraction data of the (a) pristine CBO and (b) 2%C-, (c) 4%C-, (d) 6%C- (e) 8%C- and (f)10%C-doped CBO solid solution using standard card (JCPDS file No. 34–0394 of CeO_2). The observed calculated profiles are shown by open circle solid line curves. The short vertical marks represent the Bragg diffractions. The lower curve (blue lines) is the difference plot. (a', b', c', d', e' and f') are reciprocal lattice bravicis and (a'', b'', c'', d'', e'' and f'') are atomic arrangement in unit cell with blue, green, yellow, red, crayan, and purple circle represents the elements :Bi, Ce, C, O, O and O, respectively.

Table S1. Lattice parameters observed from Rietveld refined XRD patterns along the cubic FCC structure with cell parameter a, unit cell volume and z=4 coupled with refinement fitting parameters (R_{Bragg}, χ^2) experimental chemical composition (observed from EDX) and stiochiometric compositions of the studied solid solutions**.**

Sl. No.	Sample	Lattice Parameter a (Å)	Unit Cell Volume V(Å^3)	M_w	R_{Bragg}	χ^2	Porosity $(1-\rho_b/\rho x)\times 100$ %	Experimental Composition $Ce_{0.49}Bi_{0.38}O$	Stiochiometric Composition $CeBi_2O_5$
1.	Pure CBO	5.4486(21)	161.75(11)	233.24	4.11	1.17	24.60	$Ce_{0.49}Bi_{0.38}O$	$CeBi_2O_5$
2.	2%C-CBO	5.4143(09)	158.72(5)	209.23	9.62	1.60	17.48	$C_{0.21}$ -$Ce_{0.94}Bi_{0.28}O$	$C_{0.02}$ $CeBi_2O_{4.98}$
3.	4%C-CBO	5.4140(05)	158.69(3)	223.45	6.95	1. 49	22.78	$C_{0.23}$ -$Ce_{0.98}Bi_{0.32}O$	$C_{0.04}$ $CeBi_2O_{4.96}$
4.	6%C-CBO	5.4131(05)	158.62(2)	925.63	8.18	1.69	81.37	$C_{0.95}$ -$Ce_{4.99}$ $Bi_{0.94}O$	$C_{0.06}$ $CeBi_2O_{4.94}$
5.	8%C-CBO	5.4093(10)	1.58.28(5)	214.81	9.57	1. 73	19.89	$C_{0.77}$ -$Ce_{1.05}$ $Bi_{0.10}O$	$C_{0.08}$ $CeBi_2O_{4.92}$
6.	10%C-CBO	5.4071(12)	158.09(6)	201.82	9.21	1. 80	15.15	$C_{1.47}$ -$Ce_{1.07}$ $Bi_{0.04}O$	$C_{0.10}$ $CeBi_2O_{4.90}$

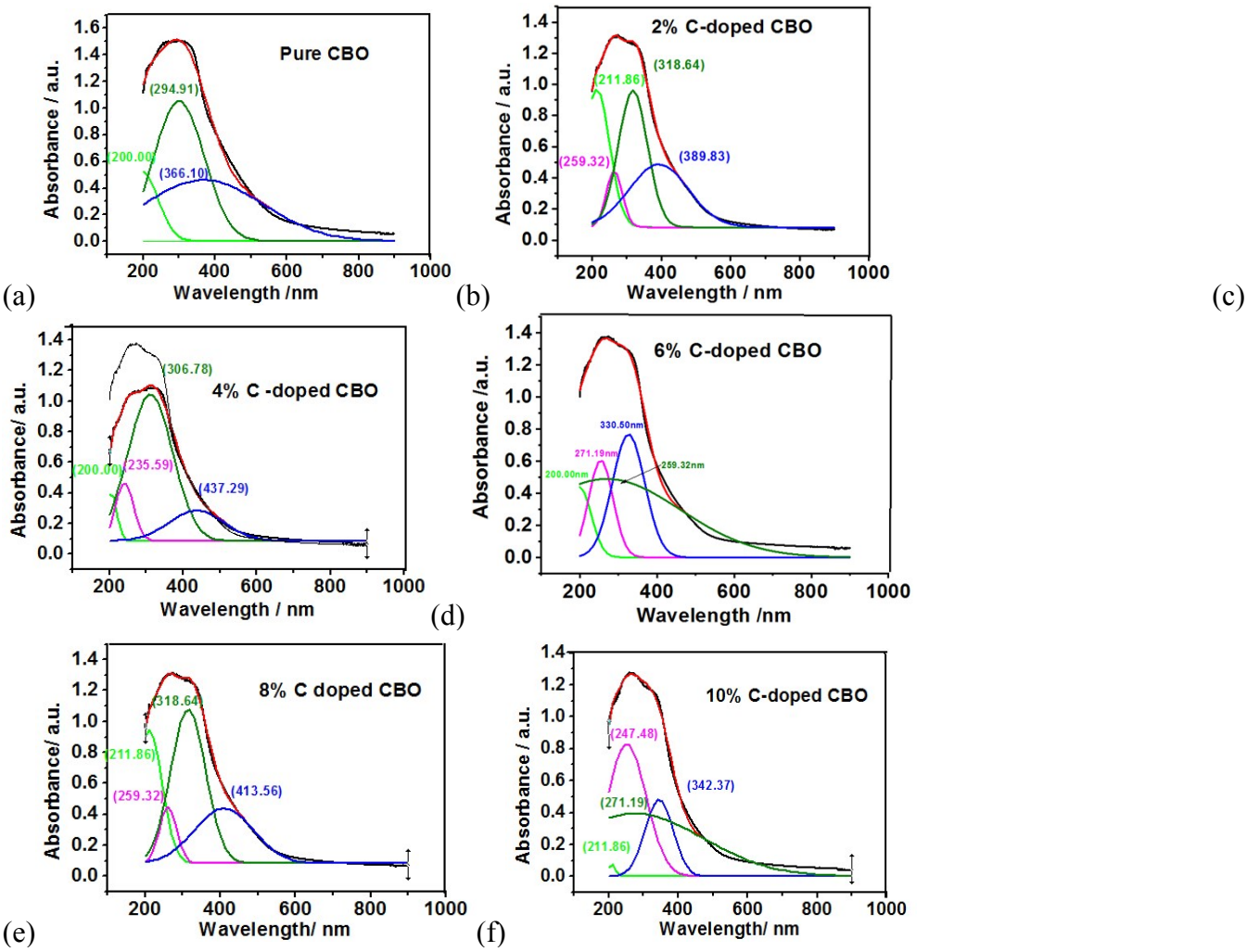

Figure S5. UV Vis spectra deconvulated into four peaks around the wavelengths (i)200-224 nm, (ii)259 nm, (iii)318 nm and (iv)342-413 nm of the solid solution (CBO)- loaded with different amount of carbon i. e. (a) 0% C, (b) 2% C, (c) 4% C, (d) 6% C, (e) 8% C, and (f) 10% C.

Table S2 Deconvulated UV-Vis spectral bands, belongs to the Ce^{3+} ion at 200-224 nm, interface between ceria and bismuth oxide (*charge transfer band*) around 259 nm, Ce^{4+} ion 318 -342 nm and Bi^{3+} ion at 425-449 nm along with the calculated direct and indirect band gap of the C-doped and pure solid solutions.

Sl. No.	Compound	direct Band gap (eV)	Indirect Band gap(eV)	Ce^{3+} band	Charge transfer band	Ce^{4+} band	Bi^{3+} band
1.	Pure CBO	2.56	2.00	200.00	---	294.91	366.01
2.	2% C-CBO	2.72	2.52	211.86	259.32	318.64	389.83
3.	4% C-CBO	2.59	1.97	200.00	235.55	306.78	437.29
4.	6% C-CBO	2.69	2.42	200.00	259.32	271.19	330.50
5.	8% C-CBO	2.79	2.50	211.86	259.32	318.64	413.56
6.	10% C-CBO	2.74	2.51	211.86	247.48	---	342.37

Note: NM, means Peak found but maxima not visible in the measurable range.

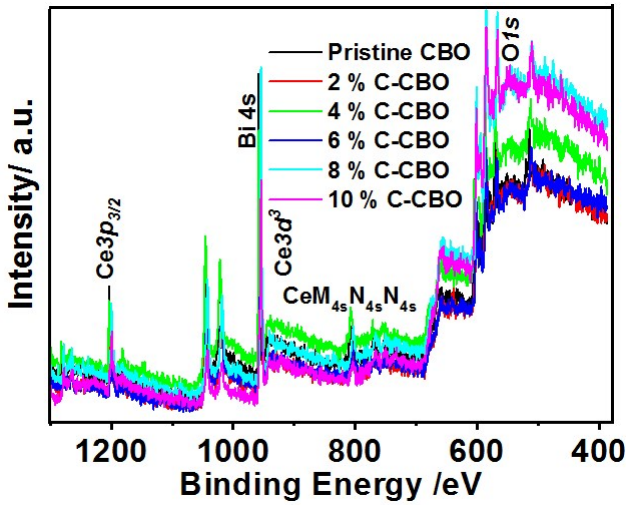

Figure S6. XPS survey-scan of the Pristine and Carbon doped CBO solid solution.

Table S3. Atomic compositions (at.%) with their respective XPS core level binding energies (eV) along the Ce $3d_{3/2}$ and Ce $3d_{5/2}$ photoelectron peaks collected for the for Pure CBO and carbon doped CBO (x = 2%, 4%, 6%, 8% and 10 %) solid solutions and stiochiometric ratio x= [O]/[Ce]= 3/2{Ce^{3+}}+2{Ce^{2+}}of the oxygen with respect to the cerium (Ce^{3+} and Ce^{+4}).

Sample	Ce $3d_{5/2}$ [eV]					Ce $3d_{3/2}$ [eV]					Ce^{3+} %	Ce^{4+} %	Ce^{3+}/Ce^{4+}	x = [O]/[Ce]	Ov
	v_0 Ce^{3+}	v Ce^{4+}	v' Ce^{3+}	v'' Ce^{4+}	v''' Ce^{4+}	u_0 Ce^{3+}	u Ce^{4+}	u' Ce^{3+}	u'' Ce^{4+}	u''' Ce^{4+}					

Pure CeO_2	881.9	883.04	884.61	888.47	897.97	898.02	900.54	901.07	907.79	916.47	19.33	80.67	0.24	0.50	1.50
2%C CBO	880.9	883.60	885.40	889.89	896.18	899.77	901.57	904.26	908.75	917.74	51.48	48.52	1.06	0.58	1.42
4%C CBO	882.1	883.90	888.45	889.35	898.34	900.13	901.93	906.42	908.22	917.2	11.37	88.63	0.13	0.75	1.25
6%C CBO	881.1	882.96	884.76	888.35	898.23	898.36	900.93	903.62	907.21	917.1	22.27	77.73	0.29	1.20	0.80
8%C CBO	881.2	882.19	884.88	888.48	896.56	898.36	901.05	902.85	907.34	916.33	34.84	65.16	0.53	0.54	1.46
10%C CBO	879.3	882.06	884.75	887.45	894.64	898.23	900.92	902.72	905.42	915.3	40.92	59.08	0.69	0.65	1.35

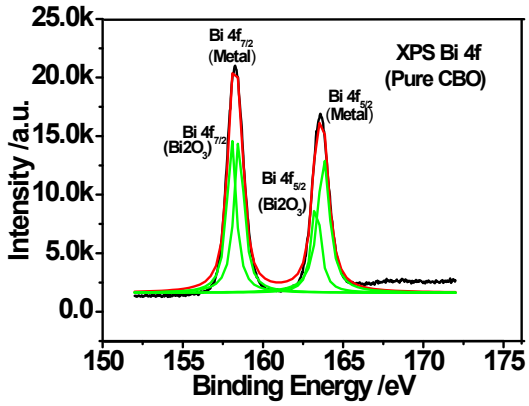

(a)

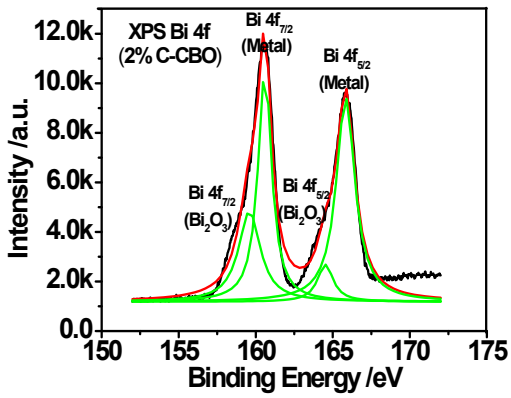

(b)

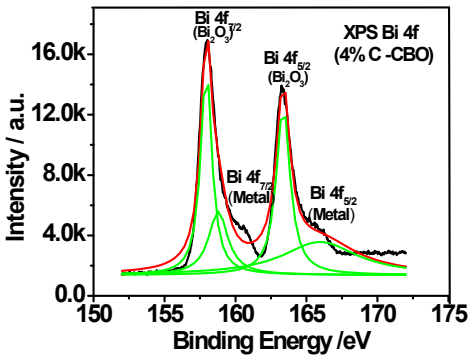

(c)

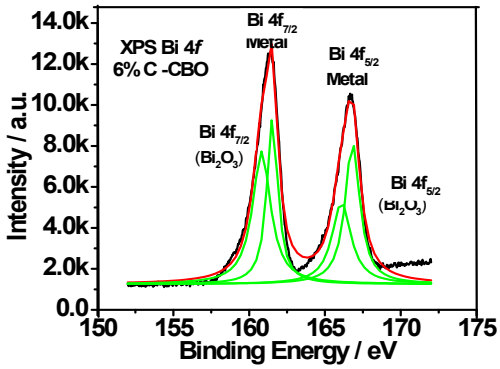

(d)

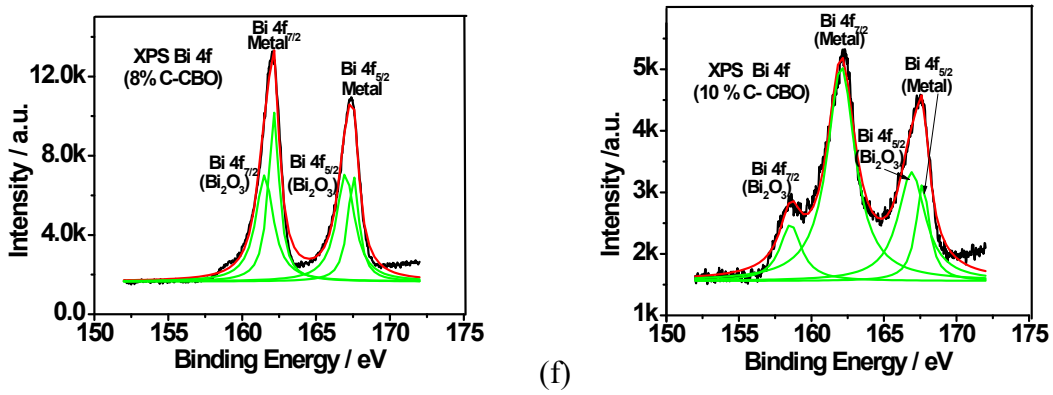

Figure S7. Deconvolution of XPS core level spectra of Bi *4f* with increase in carbon content in solid solution the Bi/O ratio. The each of the Bi *4f* $_{7/2}$ and Bi *4f* $_{5/2}$ peaks further divided in doublets represents Bi^{3+} ions and Bi metal contribution in solid solutions.

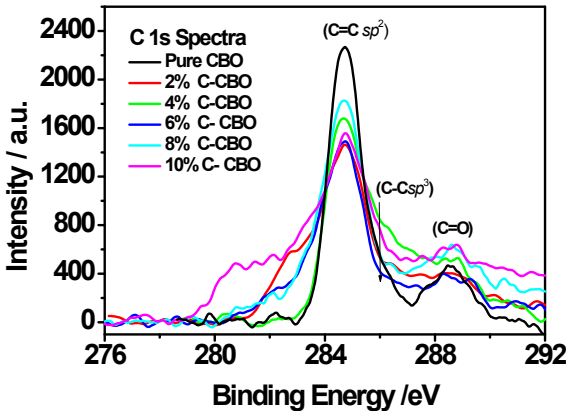

Figure S8. C *1s* core level XPS spectra for CBO solid solutions.

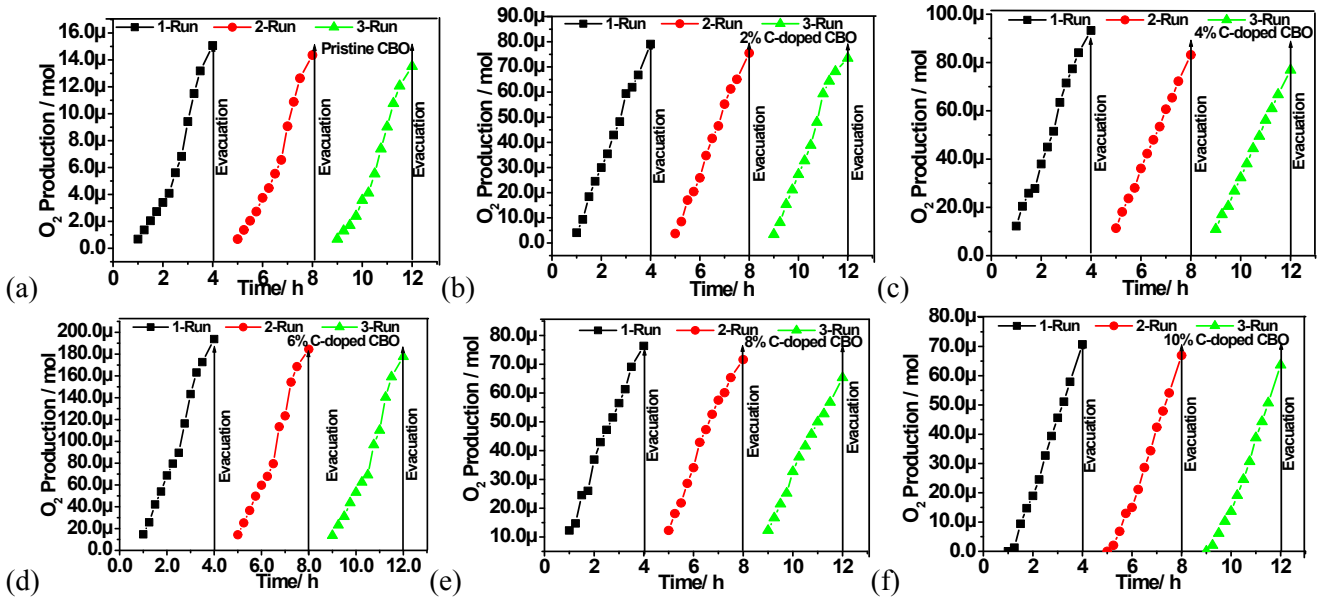

Figure S9. O_2 production during the overall water splitting of pure water under real Sun exposure for 3h at ambient conditions. Conditions: 300mg photocatalyst in 120mL DIW.

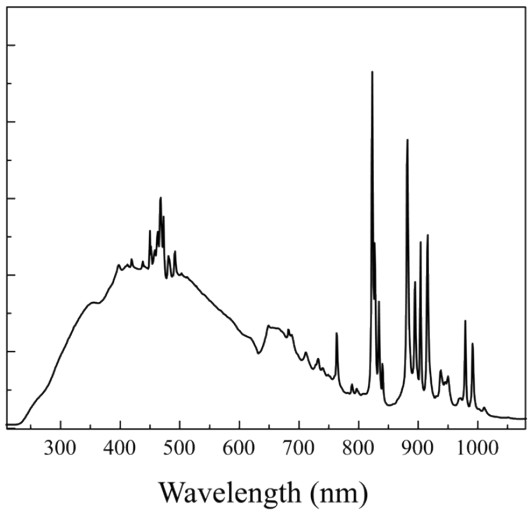

Figure S10. Spectral image of light spectra of the 300 W Xe lamp used for the H_2 production study, as provided by the vendor.

Table S4. State of art porous systems used for hydrogen generation via water splitting with their respective amount, sacrificial agent used, co-catalyst, light source, H_2 production, O_2 production, reference number, and year of publication.

Sl No.	Sample	Amount	Sacrificial agent	Co-catalyst	Toxicity	Light source	H_2 production	O_2 production	Ref.	Year
1.	Pt-Zn_3P_2-CoP (MOF)	100mg in 100mL	10% CH_3OH	5% Pt	toxic (Zn_3P_2 and CoP is Acute toxic)	Xe lamp (300 W)	9.15 mmol h^{-1} g^{-1}	--	1	2017
2.	P-doped $Zn_xCd_{1-x}S$ solid solutions	1mg in 5 mL pure water	Nil	Nil		White LED light sources (30 × 3 W)	419 μmol h^{-1} g^{-1}	--	2	2018
3.	$Ce_{0.3}Zr_{0.7}O_{1.88}N_{0.12}$ solid solution	50mg in 50 mL	(0.35 M Na_2S-0.25 M Na_2SO_3) Or NaI solution	RuO2/C ZON and Pt/WO3		300-W xenon	19 μmol and 101.7 μmol under visible light (λ > 420 nm) and UV-vis light (λ > 300 nm) irradiation		3	2018
4.	$AgTaO_3$-$SrTiO_3$ solid solutions	100mg in 100mL	Na_2SO_3 (0.05 M) hole scavenger /silver nitrate (0.05 M) e-scavenger	Pt		full range illumination (λ ≥ 250 nm) visible light illumination (λ ≥ 400 nm).	~215.2 μmol/h (λ ≥ 250 nm) and ~ 5.8 μmol/h (λ ≥ 400 nm) illumination,	---	4	2019

5.	3D g-C_3N_4 Nanosheets	50 mg in 100 mL	Nil	1 wt% Pt and 3 wt% IrO_2 as co-catalysts	nontoxic	300 W Xe lamp with a cutoff filter (λ ≥ 420 nm,	101.4 μmol h^{-1} g^{-1}	49.1 μmol g^{-1} h^{-1}	5	2019
6.	CdS/C_3N_4 (10% CCN)	----	-	Pt	CdS is toxic	visible light irradiation (λ ≥ 400 nm)	13.1 mmol h^{-1} g^{-1}	-	6	2017
7.	Pt/porous b-TiO_2 nanoflute	1 mg in 20mL deionized water (Ar)	-	0.95%Pt		Hg lamp irradiation (λ ≥ 300 nm, 500 W,	9.8 ± 0.6 μmol mg^{-1} h^{-1}	-	7	2020
		1 mg in 20mL Sea water	-	0.95%Pt			7.2 and 3.6 μmol mg^{-1} h^{-1} under UV & natural sunlight, respectively			
8.	CdS/MoS_2(6.39 wt%) /Mo sheets hybrid	10 mg in 100 mL	0.35 M Na_2S and 0.25 M Na_2SO_3.	2%Pt	CdS is toxic	300 W Xe arc lamp with UV cutoff filter	4540 μmol h^{-1} g^{-1}	-	8	2017
9.	Si/$MgTiO_3$ heterostructures	20 mg in 100 mL	Nil	No co-coatalyst		350 W Xe arc lamp.	159.33 μmol h^{-1} g^{-1}	-	9	2016
10.	CuS/ZnS	50 mg in 100mL	0.35 M Na_2S & 0.25 M Na_2SO_3	No co-coatalyst	CdS is toxic	300 W Xe arc lamp with 400 nm cut-off filter	4147 μmol h^{-1} g^{-1} (2 mol % CuS)	-	10	2011
11.	Pd@CdS /PdS	10 mg in 50 mL	0.1 M Na_2S & 0.1 M Na_2SO_3	Pd	CdS and PbS are toxic	300 W Xe arc lamp with 420 nm cut-off filter	144.8 mmol h^{-1} g^{-1}	-	11	2018
	12. ZIF-67-derived CoP particle/ g-C3N4	30 mg in 50 mL	10 vol% triethanolamine (TEOA) aqueous solution	ZIF-67-derived CoP particle	Nontoxic	300 W Xe arc lamp with 420 nm cut-off filter	201.5 μmol g^{-1} h^{-1}	-	12	2018
13.	C-doped CeO_2:Bi_2O_3 solid solution	300 mg in 120 mL	20% CH_3OH (pH=7)	0.5%Pt	Nontoxic	300 W Xe arc lamp with 420 nm cut-off filter	5413.1 μmol $g^{-1}h^{-1}$	-	This work	2021
14.	C-doped CeO_2:Bi_2	300 mg in 120	Pure water	0.5%Pt	Nontoxic	Real sunlight	323.0 μmol H_2 h^{-1} g^{-1}	161.5 μmol O_2 h^{-}	This work	2021

O_3 solid solution	mL		^{1} g^{-1}

References

1. M. Lan, R. M. Guo, Y. Dou, J. Zhou, A. Zhou, J. R. Li, Fabrication of porous Pt-doping heterojunctions by using bimetallic MOF template for photocatalytic hydrogen generation, Nano Energy 33 (2017) 238-246. [DOI: https://doi.org/10.1016/j.nanoen.2017.01.046]

2. H. F. Ye, R. Shi, X. Yang, W. F. Fu, Y. Chen, P-doped $Zn_xCd_{1-x}S$ solid solutions as photocatalysts for hydrogen evolution from water splitting coupled with photocatalytic oxidation of 5-hydroxymethylfurfural, Appl. Catal. B 233 (2018) 70-79. (DOI https://doi.org/10.1016/j.apcatb.2018.03.060)

3. Y. L. Wang, J. M. Jin, Y. H. Li, X. L. Wang, B. Zhang, X. Gong, H. F. Wang, A.P. Chen, L. R. Zheng, P. Hu, H.G. Yang, $Ce_{0.3}Zr_{0.7}O_{1.88}N_{0.12}$ solid solution as a stable photocatalyst for visible light driven water splitting, Appl. Catal. B 224 (2018) 733-739. (DOI: https://doi.org/10.1016/j.apcatb.2017.11.012)

4. J. Yu, L. Zhang, J. Qian, Z. Zhu, S. Ni, G. Liu, X. Xu, In situ exsolution of silver nanoparticles on $AgTaO_3$-$SrTiO_3$ solid solutions as efficient plasmonic photocatalysts for water splitting, Appl. Catal. B *256* (2019) 117818. (DOI: https://doi.org/10.1016/j.apcatb.2019.117818)

5. X. Chen, R. Shi, Q. Chen, Z. Zhang, W. Jiang, Y. Zhu, T. Zhang, Three-dimensional porous g-C_3N_4 for highly efficient photocatalytic overall water splitting, Nano Energy 59 (2019) 644-650. [DOI: https://doi.org/10.1016/j.nanoen.2019.03.010]

6. J. He, L. Chen, Z. Q. Yi, D. Ding, C. T. Au, S. F. Yin, Fabrication of two-dimensional porous CdS nanoplates decorated with C_3N_4 nanosheets for highly efficient photocatalytic hydrogen production from water splitting, Catal. Commun. 99 (2017) 79-82. [DOI: https://doi.org/10.1016/j.catcom.2017.05.029]

7. S. Cao, T. S. Chan, Y. R. Lu, X. Shi, B. Fu, Z. Wu, H. Li, K. Liu, S. Alzuabi, P. Cheng, M. Liu, T. Li, X. Chen, L. Piao, Photocatalytic pure water splitting with high efficiency and value by Pt/porous brookite TiO_2 nanoflutes, Nano Energy 67 (2020) 104287. [DOI: https://doi.org/10.1016/j.nanoen.2019.104287]

8. L. Zhao, J. Jia, Z. Yang, J. Yu, A. Wang, Y. Sang, W. Zhou, H. Liu, One-step synthesis of CdS nanoparticles/MoS_2 nanosheets heterostructure on porous molybdenum sheet for enhanced photocatalytic H_2 evolution. Appl. Catal. B 210 (2017) 290-296. [DOI: https://doi.org/10.1016/j.apcatb.2017.04.003]

9. W. Zhu, D. Han, L. Niu, T. Wu, H. Guan, Z-scheme Si/$MgTiO_3$ porous heterostructures: Noble metal and sacrificial agent free photocatalytic hydrogen evolution, Int. J. Hydrog. Energy 41(33) (2016) 14713-14720. [DOI: https://doi.org/10.1016/j.ijhydene.2016.06.118]

10. J. Zhang, J. Yu, Y. Zhang, Q. Li, J. R. Gong, Visible light photocatalytic H_2-production activity of CuS/ZnS porous nanosheets based on photoinduced interfacial charge transfer, Nano Letters 11(11) (2011) 4774-4779. [DOI: https://doi.org/10.1021/nl202587b]

11. Q. Sun, N. Wang, J. Yu, J. C. Yu, A hollow porous CdS photocatalyst, Adv. Mater. 30(45) (2018) 1804368. [DOI: https://doi.org/10.1002/adma.201804368]

12. X. J. Sun, D.D. Yang, H. Dong, X.B. Meng, J. L. Sheng, X. Zhang, J. Z. Wei, F. M. Zhang, ZIF-derived CoP as a cocatalyst for enhanced photocatalytic H_2 production activity of g C_3N_4, Sustainable Energy & Fuels *2*(6) (2018) 1356-1361. [DOI: https://doi.org/10.1039/C8SE00063H]